Vitrification and devitrification during the non-isothermal cure of a thermoset. Theoretical model and comparison with calorimetric experiments.

Iria Fraga, Salvador Montserrat and John M. Hutchinson*

Departament de Màquines i Motors Tèrmics, ETSEIAT, Universitat Politècnica de Catalunya, Colom 11, 08222 Terrassa, Spain

*Author for correspondence: J. M. Hutchinson, Tel: +34 93 739 8748, Fax: +34 93 739 8101, e-mail: hutchinson@mmt.upc.edu

Key words: thermoset, vitrification, devitrification, non-isothermal cure, TMDSC, TOPEM

Summary

The processes of vitrification and devitrification that occur during the non-isothermal cure of a cross-linking system are studied in terms of their dependence on frequency. Experimental results are obtained by TOPEM®, a new multi-frequency temperature modulated DSC technique, and a simulation with MATLAB was used to model the vitrification and devitrification times as a function of the frequency and heating rate. Simulations were made for five different velocities of scan. Other parameters, such as the exponents in the Kamal equation, λ in the DiBenedetto equation, and the activation energy for the frequency dependence of T_g, were also considered. The experimental and

simulated results were found to be in good agreement and some advantages of the TOPEM technique are discussed.

Introduction

During the cure of thermosetting resins, the glass transition temperature of the system, T_g, changes from its initial value, T_{g0}, namely that of the unreacted mixture, and increases with increasing degree of cure, α. In a non-isothermal cure experiment, the cure temperature increases at a constant rate. If this rate is sufficiently high, the cure temperature is always higher than the T_g of the reacting system, so the cross-linking reaction will proceed to its limit, α=1, and the final glass transition temperature will be that of the fully cured thermoset, $T_{g\infty}$. On the other hand, if the curing process takes place at a sufficiently slow heating rate, the T_g of the reacting system can reach the instantaneous cure temperature, whereupon the system changes to a glassy state and vitrifies, analogous to the case of isothermal curing at sufficiently low cure temperatures.[1,2] The subsequent process of devitrification occurs when the continually increasing cure temperature, T_c, again exceeds the T_g of the vitrified system.

The vitrification and devitrification processes which occur during non-isothermal cure have been studied by temperature modulated differential scanning calorimetry (TMDSC) [3-6] and other dynamic techniques such as dielectric relaxation [7] and torsional braid analysis. [8] The advantage of these dynamic techniques is that they permit the observation of vitrification and devitrification in real time during the experiment, for example through the complex heat capacity in TMDSC. Nevertheless, a limitation of these TMDSC measurements is that they have until now been restricted to

a single frequency in any one experiment, typically with a period of 60 s. Since the underlying heating rate is slow, these experiments tend to be time-consuming, often requiring up to 10 hours, with the consequence that the effect of frequency has not been investigated. One of the purposes of the present work is to study, by a temperature modulated calorimetric technique, the frequency dependence of the vitrification and devitrification processes during the non-isothermal cure of an epoxy-diamine system.

In the first part of this work, we make use of TOPEM to investigate these processes experimentally. TOPEM is based on the application of stochastic temperature pulses superimposed on the underlying constant heating rate, which allows the evaluation of the response over a wide range of frequencies in a single experiment, [9] for example for the study of the kinetics of the glass transition.[10,11] In the second part of this work, we make use of a theoretical simulation to obtain the vitrification and devitrification times as a function of frequency in order to compare them with the experimental results.

Experimental

Materials

The epoxy resin used was a diglycidyl ether of bisphenol-A (DGEBA), Epon 828 (Shell Chemicals). The cross-linking agent was a polyoxypropylene diamine, Jeffamine D-230 (Huntsman Corporation). Stoichiometric mixtures of resin and diamine were prepared immediately prior to each experiment and samples of suitable mass, around 25 mg, were weighed and sealed into aluminium crucibles.

Methods

A Mettler-Toledo 823^{e} calorimeter with an intracooler was used for the experiments. The TOPEM software incorporated in the calorimeter controls the stochastic temperature pulses that are superimposed upon the underlying heating rate of the conventional non-isothermal scan, and subsequently evaluates the response, including the separation of selected frequency components. In any single scan, the temperature amplitude of the pulses is fixed while the duration of the pulses is random, between two values, minimum and maximum, called the "switching time range". [9] All of these experimental parameters are selected by the user.

Non-isothermal scans between 25ºC and 100 – 125ºC, the final temperature depending on the underlying heating rate, were made. The underlying heating rates selected were 0.05, 0.032, 0.025, 0.019 and 0.015 K/min, which are sufficiently slow to observe the vitrification and devitrification processes clearly separated. For comparison, a velocity of 0.1 K/min was also investigated, and no vitrification was observed. For all the experiments a temperature amplitude of the pulses of 0.1 K was selected, with the switching time range being from 15 s to 30 s.

Conventional non-isothermal DSC scans were also made in order to investigate the partial cure of the samples in respect of their glass transition temperature and the degree of cure reached at vitrification. The heating rates selected were the same as for the TOPEM experiments, namely between 0.05 and 0.015 K/min, and the temperature ranges for the scans were from 25ºC to the temperature of vitrification, this last being different for each heating rate and having been identified from the previous TOPEM

experiments. Second scans were made in all cases in order to determine the residual heat of reaction, from which the degree of cure at vitrification is found, and the glass transition temperature of the samples at vitrification. Third scans were also made to determine the glass transition temperature of the fully cured samples.

Experimental Results and Discussion

Typical results for a non-isothermal cure in TOPEM are shown in Figure 1. The upper figure shows the on-line measured heat flow response of a sample to a scan with stochastic temperature pulses superimposed on the underlying heating rate. From this response, the quasi-static heat capacity, C_{p0} and the total heat flow can be calculated, and are shown in the middle and lower figures, respectively. From the C_{p0} curve, the frequency dependent heat capacities, $C_p(f)$, at selected frequencies (f) can be calculated. The user selects the asymptotes of the vitrification and devitrification processes, as shown in Figure 1, as well as the frequencies for the determination of $C_p(f)$. [12] The different curves for $C_p(f)$ at the selected frequencies are shown in the middle figure.

The heating rate in this experiment is 0.019 K/min, sufficiently small to identify both vitrification and devitrification processes clearly separated. The vitrification can be observed in the first rather abrupt change (reduction) of the specific heat capacity, while the devitrification is observed in the second, less abrupt, change in which the specific heat capacity increases. A similar behaviour was found for all the heating rates used. The vitrification and devitrification times are taken as the times at which the specific heat capacity has a value midway between the two relevant asymptotes. The dependence on frequency of the times for vitrification and devitrification can be seen in

the middle figure, where it is interesting to observe that the effects are opposite: with increasing frequency, the vitrification time decreases whereas the devitrification time increases. It can also be seen that such small heating rates result in very time-consuming experiments: 70 h in this case. Around 350 hours were needed to complete all the experiments for this study.

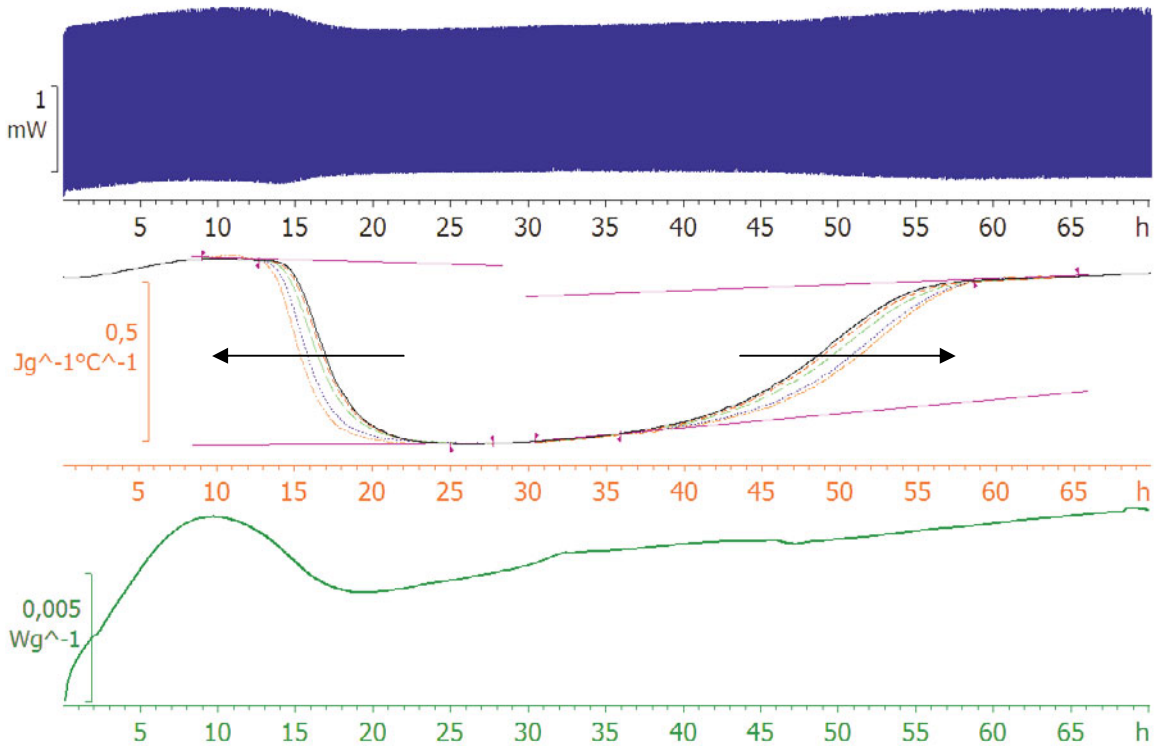

Figure 1. Heat flow response (upper), specific heat capacities at selected frequencies (C_{p0}, 8, 16, 32, 64 mHz) (middle), and total heat flow (lower) as a function of time for a TOPEM experiment from 25 to 105ºC at 0.019 K/min, with temperature pulses of amplitude 0.1 K and switching time range between 15 and 30 s. The arrows show the directions of increasing frequency.

Figure 2 shows the behaviour of the quasi-static heat capacity, C_{p0}, as a function of both time and temperature for each of the underlying heating rates used. The frequency dependent heat capacities for different frequencies are not represented here for reasons of clarity, but similar results as in Figure 1 (middle graph) could be obtained.

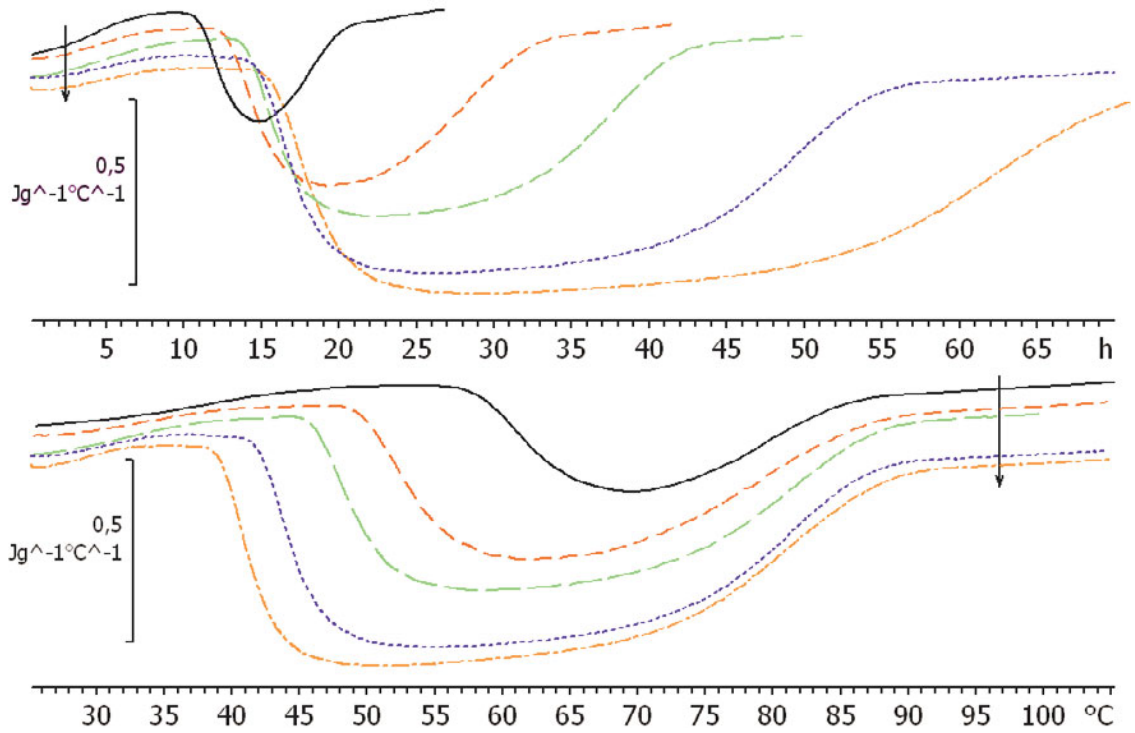

Figure 2. Quasi-static heat capacities, C_{p0}, as a function of time (upper) and temperature (lower) for each of the underlying heating rates used: 0.05 (black, full line), 0.032 (red, short dash), 0.025 (green, long dash), 0.019 (blue, dotted) and 0.015 K/min (orange, dash dotted). The arrows show the direction of decreasing heating rate.

It can be seen that for slower heating rates the two transitions appear more separated. It can also be clearly seen that the increment in specific heat capacity at vitrification, $\Delta C_{p,vit}$, increases as the heating rate decreases. According to the inverse relationship [13]

between ΔC_p and degree of cure, α, the effect of decreasing the underlying heating rate should be to result in a decrease in the degree of cure at vitrification, α_{vit}. The degree of cure at vitrification for each underlying heating rate is obtained from:

$$\alpha = \frac{\Delta H_v}{\Delta H_{total}} \quad (1)$$

where ΔH_v is the heat of reaction evolved up to vitrification and ΔH_{total} is the total heat of reaction corresponding to the complete process of cure. These heats of reaction are determined from conventional DSC scans in the manner described above.

The results obtained for both $\Delta C_{p,vit}$ and α_{vit} are shown in Table 1. Although an inverse relationship between $\Delta C_{p,vit}$ and α_{vit} is apparently followed here, a closer inspection reveals that the situation is more complicated. In particular, given that ΔC_p for the fully cured resin, obtained as an average following second and third scans after partial curing until vitrification at each of the underlying heating rates, is 0.484 ± 0.010 J/gK, there is an inconsistency in that several of the values of $\Delta C_{p,vit}$ in Table 1, which apply to partially cured resins, are less than this value for the fully cured resin. The explanation of this, as pointed out earlier by Van Mele and co-workers [3,4] who analysed the vitrification and devitrification processes by means of the diffusion factor concept, is that the vitrification is only partial, and particularly so for the higher heating rates. This can clearly be seen by a comparison of the $\Delta C_{p,vit}$ values from TOPEM in Table 1 with those obtained from the second scans by conventional DSC of the partially cured resins: for example, for heating rates of 0.05, 0.032 and 0.015 K/min, these latter values are 0.580, 0.615 and 0.624 J/gK, respectively. Thus complete vitrification does not occur, except possibly for the slowest heating rate used here (0.015 K/min), for which there is only a small difference between the $\Delta C_{p,vit}$ values obtained by TOPEM (0.601 J/gK) and

by DSC (0.624 J/gK). This difference is likely to arise from the DSC value being obtained after curing only to the mid-point of the ΔC_p step (vitrification time), where the degree of cure is slightly less than at the end of the step, implying a slightly higher value of ΔC_p. Furthermore, the wide separation of the vitrification and devitrification processes in Figure 2 for this heating rate, and the establishment of an apparently glassy baseline between them, would lead one to believe that the vitrification was complete in this case.

Table 1. Specific heat capacity increment, $\Delta C_{p,vit}$, and degree of cure, α_{vit}, at vitrification for each underlying heating rate.

underlying heating rate K/min	**$\Delta C_{p,vit}$ J/gK**	**α_{vit}**
0.05	0.287	0.870
0.032	0.428	0.788
0.025	0.482	0.734
0.019	0.565	0.682
0.015	0.601	0.626

The vitrification and devitrification times and temperatures are determined from the two sigmoidal changes observed in the curves of the specific heat capacities for each frequency. The frequency dependence of the vitrification temperature is shown in Figure 3, where it can be seen that it decreases with increasing frequency and that, as can also be seen in Figure 2, the system vitrifies at higher temperature the higher is the

underlying heating rate. Although not shown here, the vitrification time also decreases with increasing frequency and, as in the case of isothermal cure of the same system, [2] there is again a non-linear relationship between vitrification time and log(frequency). In contrast to the vitrification temperature, though, the system vitrifies at shorter times the higher is the underlying heating rate, an effect seen also in Figure 2.

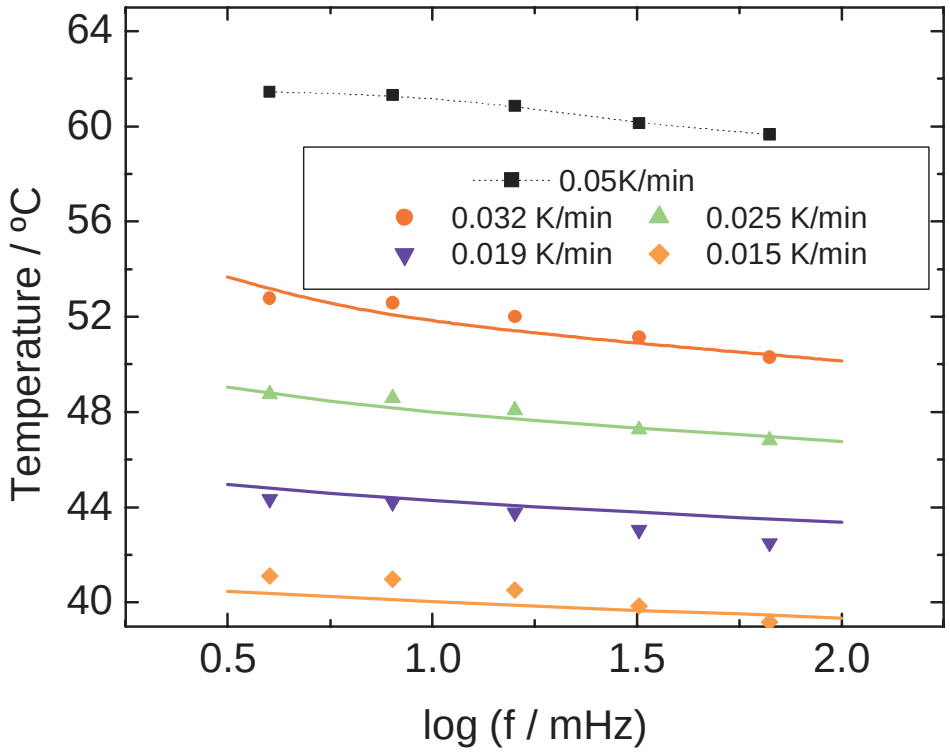

Figure 3. The points represent the vitrification temperature as a function of frequency, on a logarithmic scale, obtained from TOPEM experiments with underlying heating rates from 0.05 K/min to 0.015 K/min, as indicated. The full lines represent the model predictions using the following parameter values: m= 1.24, n=1.7, λ=0.15 and E_f/R =150 kK. The dotted line for the heating rate of 0.05 K/min is only a guide for the eye.

In the case of the devitrification process, as is shown in Figure 4, the dependence of the devitrification time on frequency is the opposite of that found for vitrification, in that the devitrification time increases with increasing frequency. The dependence of the devitrification time on frequency is also less pronounced than in the case of vitrification, while, as can be seen in Figure 2, the devitrification temperature is almost independent of the underlying heating rate.

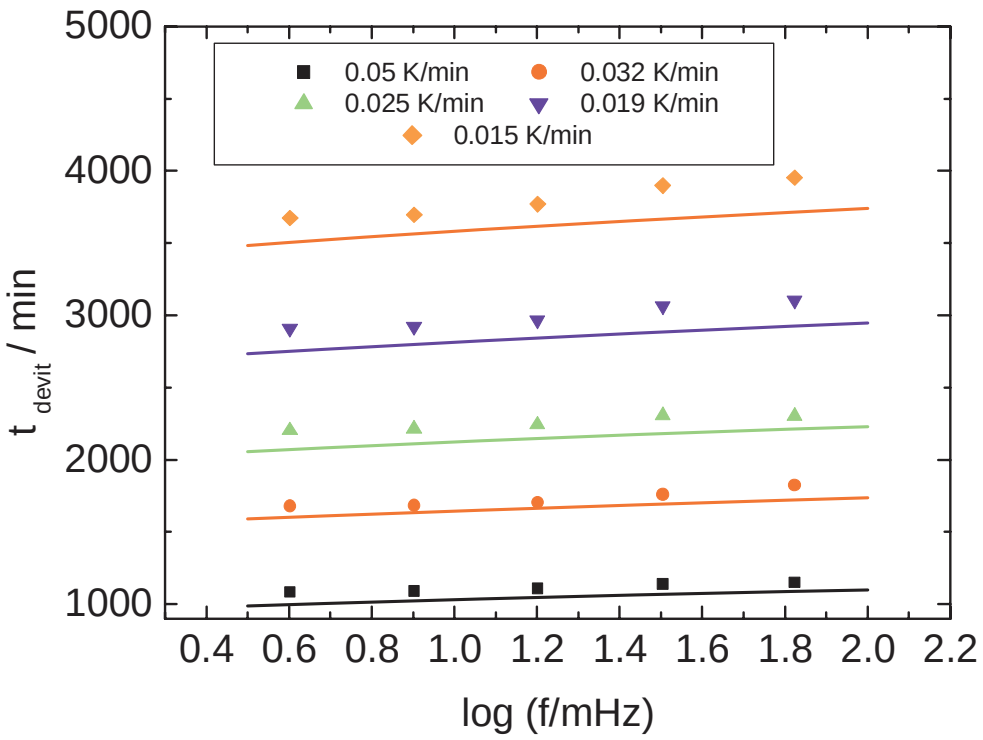

Figure 4. Points represent the devitrification time versus frequency, on a logarithmic scale, obtained from TOPEM experiments with underlying heating rates from 0.05 K/min to 0.015 K/min, as indicated. The full lines represent the model predictions using the following parameter values: m=1, n=1.5, λ=0.5 and E_f/R =150 kK.

With the results obtained from TOPEM experiments for the vitrification and devitrification times, a Continuous Heating Transformation (CHT) diagram, analogous to the TTT diagram in the isothermal case, can be constructed, [5-8] and is shown in Figure 5. In this diagram, the vitrification and devitrification times for five selected frequencies have been included: 4.33 mHz, 8.33 mHz, 16.67mHz, 33.33mHz and 66.66 mHz. The underlying heating rates for the non-isothermal cures and the glass transition temperature of the fully cured system, obtained from second scans, are also shown. From this diagram one can obtain information about the vitrification and devitrification regions, and their dependence on time, heating rate and frequency.

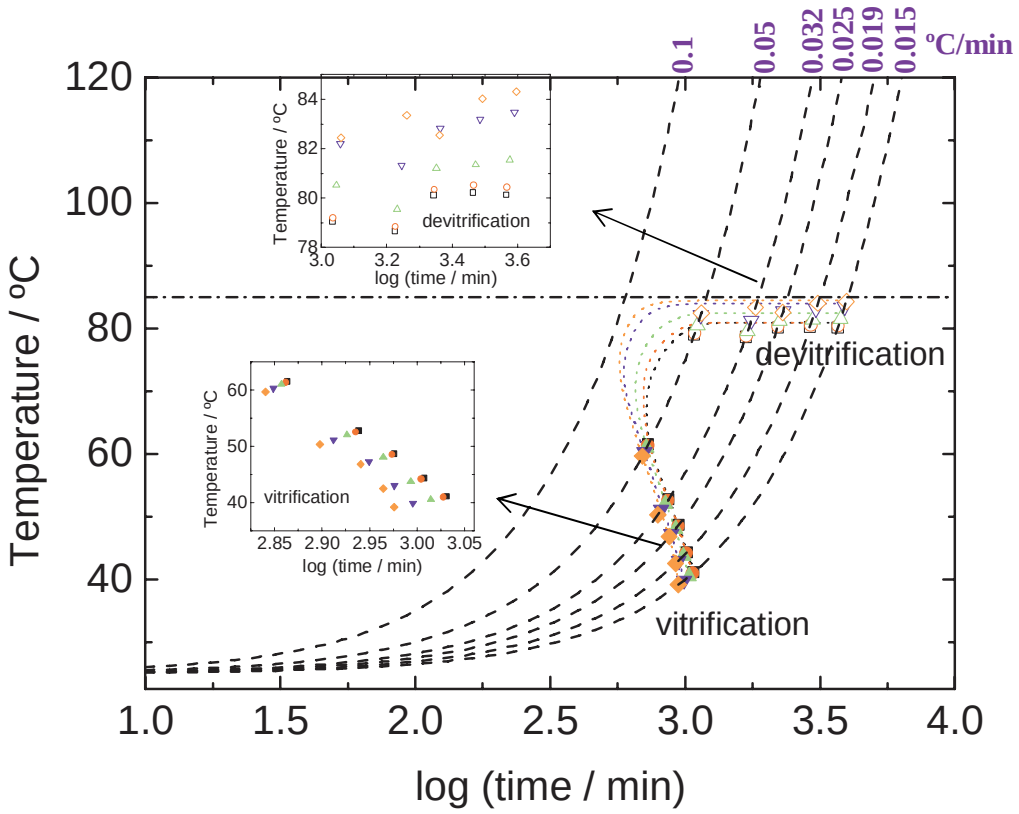

Figure 5. Continuous Heating Transformation (CHT) cure diagram for the system. The experimental points indicate vitrification (filled points) and devitrification (unfilled points) times, the dashed lines show the underlying heating rates as indicated, and the dash-dotted line represents the glass transition temperature of the fully cured system. The insets give an enlarged view of the vitrification and devitrification processes. Dotted lines are only a guide for the eye. The frequencies selected are: 4.33 (black squares), 8.33 (red circles), 16.67 (green triangles), 33.33 (blue inverted triangles) and 66.66 mHz (orange diamonds).

Theory and Simulation

MATLAB version 7.0 was used to simulate the non-isothermal cure reaction, taking into account similar considerations as for the isothermal case. [14] In the absence of vitrification, the reaction is chemically controlled and the time (t) dependence of the degree of cure (α, $0 \leq \alpha \leq 1$) during the reaction can be described by the equation of Kamal: [15]

$$\left(\frac{d\alpha}{dt}\right)_{chem} = (k_1 + k_2 \cdot \alpha^m) \cdot (1-\alpha)^n \qquad (2)$$

where k_1 and k_2 are temperature dependent rate constants, and the exponents m and n are the reaction orders, their sum usually being approximately $m+n \approx 2$. The rate constants are considered to have an Arrhenius temperature (T) dependence: [16]

$$k_{c\,(1,2)} = A_{(1,2)} \cdot \exp\,[-E_{c(1,2)} / RT\,] \qquad (3)$$

where A and E_c are pre-exponential parameters and activation energies, respectively, and R is the universal gas constant. The subscript c for k and E indicates that these are values for the chemically controlled reaction.

When vitrification occurs, the rate of cure becomes controlled by diffusion, and it is therefore necessary to introduce, in addition, a rate constant for diffusion, k_d. One possibility is to assume this rate constant to have a WLF temperature dependence: [17,18]

$$k_d = k_{dg} \cdot \exp[\, C_1(T - T_g)\,/(C_2 + T - T_g)] \qquad (4)$$

where C_1 and C_2 are constants, here assumed to take their "universal" WLF values [17] of 40.2 and 51.6 K, respectively, T_g is the glass transition temperature of the reacting system, and k_{dg} is the value of k_d when T_g is equal to the cure temperature, i.e. at vitrification. It should be pointed out that there are other possibilities for the temperature and T_g dependence of k_d, which are discussed in the previous work [14] together with a consideration of the value of k_{dg}.

The chemical and diffusion rate constants can be combined into overall rate constants, $k_{tot(1,2)}$, by means of the Rabinowitch equation: [19]

$$\frac{1}{k_{tot(1,2)}} = \frac{1}{k_d} + \frac{1}{k_{c(1,2)}} \tag{5}$$

These overall rate constants are used in place of k_1 and k_2 in the Kamal equation, Equation (2), in order to describe the rate of cure throughout the reaction, including that part in which vitrification occurs. As the reaction proceeds, the glass transition temperature increases from its initial value, T_{g0}, being that of the mixture of monomers of resin and cross-linking agent, and, in the absence of vitrification, will reach a limiting value, $T_{g\infty}$, corresponding to the fully cured system (α=1). The relationship between the degree of cure and the glass transition temperature of the curing system can be described by the DiBenedetto equation: [16,20]

$$\frac{T_g - T_{g0}}{T_{g\infty} - T_{g0}} = \frac{\lambda\alpha}{1-(1-\lambda)\alpha} \tag{6}$$

where λ is a fit parameter related to the ratio of heat capacities of the fully cured and uncured system. The effect of λ is also investigated in these simulations.

The combination of these equations is sufficient to define the dependence of the rate of cure, proportional to the heat flow measured in a typical DSC experiment, as a function of time (or of degree of cure) during a non-isothermal curing reaction. In the simulation, for each time step dt the increment in α (dα) is evaluated by Equation (2) using the current value of α. For the rate constants in Equation (2), the overall rate constants $k_{tot(1,2)}$ are used, calculated from Equation (5) in which the chemical rate constants k_c depend on the cure temperature, T_c, through Equation (3) and the diffusion rate constant k_d is determined by both T_c and the α-dependent T_g through Equation (4).

Vitrification is the process, characterised by a vitrification time or temperature, which occurs when the curing reaction cannot continue at the chemically controlled rate, defined here by Equation (2) and (3), because the controlling factor becomes the rate of diffusion of the reacting species. The change from a chemically controlled rate to a diffusion controlled rate is equivalent to a transition to a glassy state, and consequently vitrification is considered to occur here when T_g reaches the cure temperature, T_c, which is continually increasing according to the underlying heating rate. The equivalence of T_g and T_c was the standard method of investigating vitrification by DSC before the introduction of TMDSC. [1] The rate of cure dramatically slows down at vitrification, being dominated now by the diffusion rate constant, but does not stop completely. The cure continues, albeit rather slowly, and when T_g once again reaches the continuously increasing cure temperature, devitrification takes place.

Although the usual experimental evaluation of the vitrification time in TMDSC, and of the vitrification and devitrification times by TOPEM here, is from the mid-point of the sigmoidal change in the frequency dependent heat capacity, n these simulations we evaluate it as the time at which the dynamic (frequency dependent) glass transition temperature is equal to the cure temperature, equivalent to the definition of the vitrification time determined by conventional DSC.[1] For these purposes, we adopt here the same procedure as was used for the earlier study of isothermal vitrification [14] in order to simplify the analysis. This is based on the fact that it is the equivalence of T_g and T_c which is used to define vitrification, and that in reality it is T_g which has the frequency dependence, increasing with increasing frequency. However, the condition T_g=T_c would be reached in the same way if T_g were considered to be frequency-independent and a frequency dependence were instead attributed to T_c, but such that it decreased with increasing frequency. Hence, in the present analysis, the frequency dependence is assigned to the cure temperature which, in addition to increasing with time following the underlying heating rate, also decreases with increasing frequency. Thus the dynamic vitrification time occurs when T_g= $T_c(f)$, where $T_c(f)$ is the frequency dependent cure temperature, given by:

$$\ln\left(\frac{f}{f_r}\right) = \frac{E_f}{R}\left(\frac{1}{T_c(f)} - \frac{1}{T_c(t)}\right) \tag{7}$$

In this equation, E_f is the activation energy controlling the frequency dependence of T_c, and f_r is a reference frequency for which the dynamic cure temperature, $T_c(f)$, is considered to be equal to the cure temperature, T_c, which depends on time according to the underlying heating rate. Since the vitrification time determined by conventional DSC makes use of a glass transition temperature determined on heating after, typically, previously cooling freely,[1] we can use the correspondence between cooling rate and

frequency [21,22] to assign a value of 1/60 s^{-1} for the reference frequency. The effect of various values of the activation energy, E_f, is investigated in the simulation.

Figure 6 shows a typical example of how the glass transition temperature varies throughout the cure process, including vitrification and devitrification, as modelled by these simulations. The dotted line represents the variation in the glass transition temperature which occurs during cure with vitrification and subsequent devitrification, whereas the dashed line shows the hypothetical variation that would occur in the absence of vitrification. The first intersection of the curve for the changing glass transition temperature (dotted line) with the cure temperature (full line) for any frequency represents the vitrification point for that frequency, while the second intersection of the same curve represents the devitrification point for the same frequency. The parallel lines correspond to frequencies of 3.16, 16.7 and 100 mHz. For the reasons stated above, the intersection with the line for 16.7 mHz defines the vitrification and devitrification times equivalent to those which would be obtained by conventional DSC.

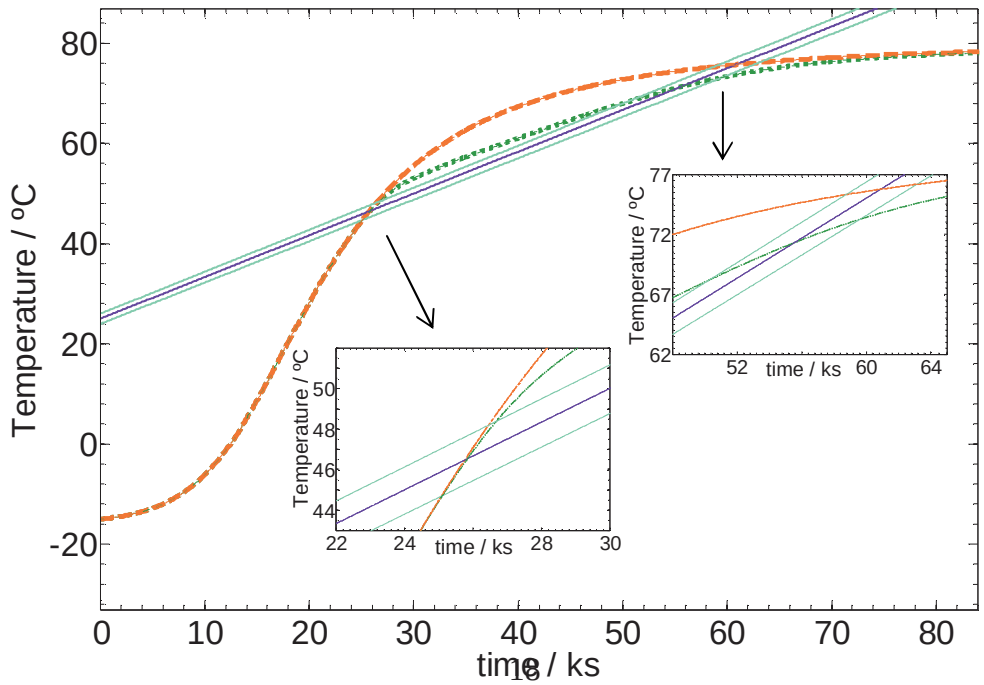

Figure 6. Increase of T_g with time during a non-isothermal cure with an underlying heating rate of 0.05K/min for a system with T_{g0}=258 K and $T_{g\infty}$=353 K in the absence of vitrification (red dashed line) and when vitrification and devitrification intervene (green dotted line). The parallel lines indicate the time dependence of the cure temperature for different frequencies: the central line for the reference frequency (1/60 s^{-1} $\leftrightarrow$16.67 mHz), the upper line for a frequency of 3.16 mHz, the lower line for a frequency of 100 mHz. The two intersections of the cure temperature lines with the T_g curve define the vitrification (first) and devitrification (second) points, which can be seen more clearly in the insets. Other parameter values for the simulation are: m=0.9, n=2, E_f/R=150 kK and λ=0.66.

The values of the constants used in these simulations are summarized in Table 2. Also shown are the ranges of parameter values investigated, namely the underlying heating rate, q, the reaction orders, m and n, in Equation (2), the parameter λ of the DiBenedetto equation, Equation (6), and the reduced activation energy, E_f/R, in Equation (7). In any one calculation, a set of parameter values is chosen. For all the results presented here, the set of values is always indicated, but in respect of trends the results shown are typical of a very large range of combinations of parameter values used in this investigation. It is only for those calculations where a fit of the model is made to the experimental data that the actual values of the parameters are important.

Table 2. Constants and ranges of parameter values used in the simulations

Constant	**Value [ref.] and equation where used**

A_1 (s^{-1})	$10^{3.6}$ [18] Equation (3)
E_{c1} (kJ mol^{-1})	51.8 [18] Equation (3)
A_2 (s^{-1})	$10^{3.4}$ [18] Equation (3)
E_{c2} (kJ·mol^{-1})	41.5 [18] Equation (3)
k_{dg} (s^{-1})	0.0051 [14] Equation (4)
C_1	40.2 [17] Equation (4)
C_2 (K)	51.6 [17] Equation (4)
T_{g0} (ºC)	-15 Equation (6)
$T_{g\infty}$ (ºC)	80 Equation (6)
Parameter	**Values**
q (K min^{-1})	0.05 0.032 0.025 0.019 0.015 0.012
m	0 0.4 0.9 0.98 1 1.24 2
n	0 1 1.12 1.43 1.5 1.6 1.7 2
λ	0.1 0.15 0.33 0.5 0.66 1
E_f/R (kK)	25 50 75 110 100 120 150

Results of Simulation

Typical results for the dependence of the vitrification temperatures and the devitrification times on log(f) for different underlying heating rates are shown in Figure 7 and 8, respectively, for frequencies from 1 mHz to 10^5 Hz. The regions of these graphs which correspond to the TOPEM experiments are at the extreme left, for log(f/mHz) in the range 0.5 to 2.0, approximately. The region at higher frequencies would correspond to other types of dynamic experiment which operate over a higher

frequency range, such as dynamic mechanical analysis (up to about 10^3 Hz) and dielectric analysis.

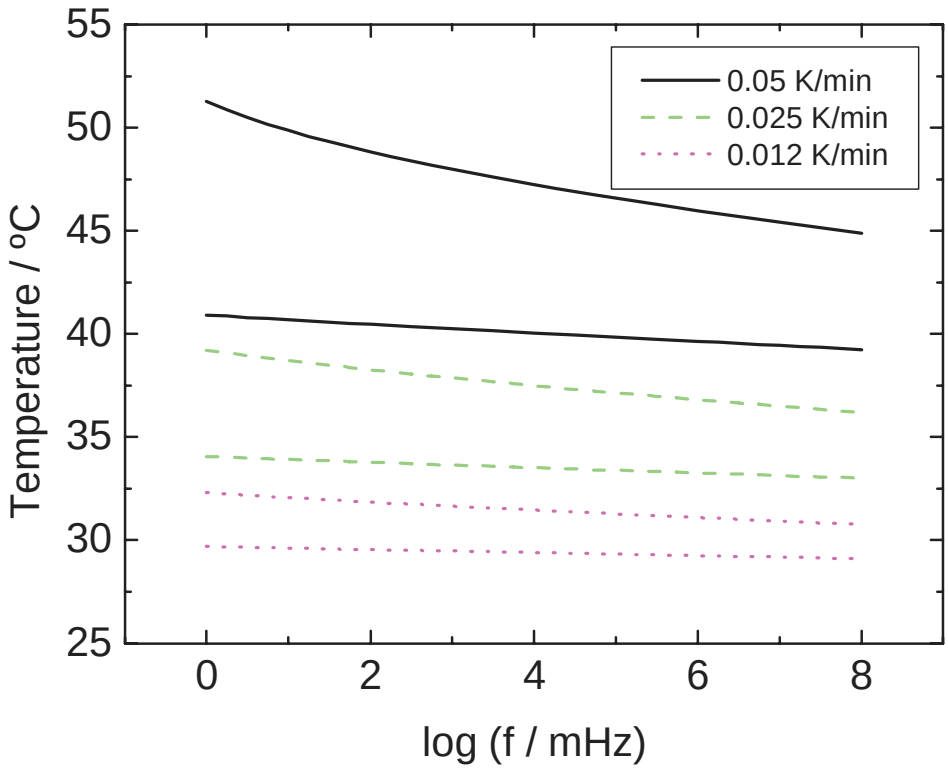

Figure 7. Frequency dependence of the vitrification temperature for three different underlying heating rates: 0.05 (black continuous lines), 0.025 (green dashed lines) and 0.012 (lilac dotted lines) K/min. The parameter values for the different simulations are: m=0.9, n=1.7, E_f/R=120 kK, λ=0.33 (upper curves); m=0.98, n=1.12, E_f/R=150 kK, λ=1 (lower curves).

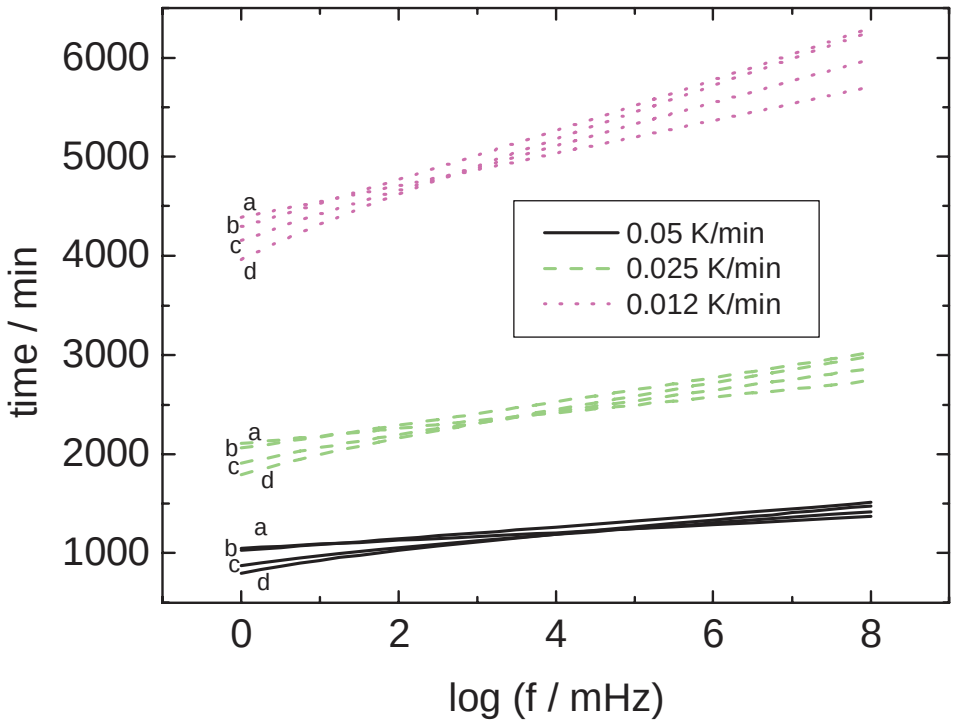

Figure 8. Frequency dependence of the devitrification time for three different underlying heating rates: 0.05 (black continuous lines), 0.025 (green dashed lines) and 0.012 (lilac dotted lines) K/min. The parameter values for the different simulations are: (a) m=0.98, n=1.12, E_f/R =150 kK, λ=1; (b) m=1, n=1, E_f/R =100 kK, λ=0.66; (c) m=0.9, n=1.7, E_f/R =120 kK, λ=0.33; (d) m=1, n=2, E_f/R =110 kK, λ=0.66.

It can be seen from Figure 7 that, in respect of the vitrification temperature, there is a noticeable dependence on the kinetic parameters (m, n, λ, E_f/R), though the general trend of a rather linear decrease of the vitrification temperature with increasing frequency is always present. In this case, the effect of changing parameter values is principally a displacement of the curves on the temperature scale, with a slight change of slope and, for the fastest underlying heating rate, the introduction of some curvature at the lowest frequencies. In contrast, the results for the devitrification time shown in Figure 8 indicate that different values for the kinetic parameters have a much less significant effect on the devitrification time, which generally displays a rather linear

increase with increasing frequency. The most significant deviation is the evidence of some curvature at the lowest frequencies., analogous to the deviation seen in this frequency range for the vitrification temperature in Figure 7 for the fastest underlying heating rate. A detailed comparison of these simulations with the TOPEM experimental results is provided in the following section.

Comparison of Simulation with TOPEM Measurements

From the simulations, it is possible to obtain results very similar to those obtained by TOPEM by adjusting the parameter values appropriately. This can be seen in Figure 3 and 4, where the vitrification temperature and the devitrification time, respectively are represented as a function of the frequency on a logarithmic scale, for both the simulated results and the earlier experimental TOPEM data. It can be seen that there is a good correspondence between simulated and experimental results, in particular with the rather linear decrease in vitrification temperature and increase in devitrification time with increasing frequency being well represented.

It will be noticed, though, that the parameter values (m, n, λ and E_f/R) are different for the fit of the simulation to the experimental data in Figures 3 and 4. It has proved impossible to model precisely the vitrification and devitrification behaviours of Figure 3 and 4 with the same set of parameter values. In particular, the experimental data fall at longer devitrification times than are predicted by simulation making use of the parameter values obtained from the vitrification data, and the discrepancy becomes increasingly larger the slower is the underlying heating rate.

An explanation for this may lie in a relaxation process taking place during the period between vitrification and devitrification. During this period in which the system is vitrified, it remains at a temperature just below the continuously changing T_g, which means that some structural relaxation will be taking place. The effect of this will be to increase the average relaxation time, with the result that the devitrification process will be delayed until a higher temperature is reached. This is just the effect observed in trying to simulate the experimental results with parameter values taken from a fit to the vitrification process. Furthermore, the relaxation that takes place during the period between vitrification and devitrification will be greater the longer is this period, which occurs for slower underlying heating rates. The effect of this will be that the delay in the devitrification will be greater the slower is the underlying heating rate, which is again just what is observed in practice. As an illustration, the slowest heating rate used here experimentally was 0.015 K/min, for which this period between vitrification and devitrification lasts about 20 hours or more (see Figure 2), which is ample time for considerable structural relaxation to occur.

These relaxation effects could be included in a considerably more complex simulation, which would require the determination of how the average relaxation time increases during the period of vitrification. The approach would be to make use of the kind of model which describes rather well the typical glassy state relaxation behaviour of polymers, for example one which incorporates parameters to model the effects of non-exponentiality (β) and non-linearity (x) on the response, [23-26] and to make use of the concept of fictive temperature, T_f, rather than T_g for evaluating the changes in the

relaxation time and in the rate constant for diffusion calculated by Equation (4). Work on this aspect of the model is planned for the future.

Conclusions

The use of TOPEM in studying the vitrification and devitrification processes during the non-isothermal cure of thermosetting resins presents a significant advantage over other temperature modulated DSC techniques, such as ADSC. A single experiment permits the evaluation of the dynamic vitrification and devitrification times and temperatures for a selected range of frequencies. This is an advantage compared with other modulated calorimetric techniques, for which a similar study would not only be very time consuming but would also necessitate the preparation of a new sample for each frequency, thus introducing the possibility of additional experimental error. The dependence of the vitrification and the devitrification processes on frequency has been studied experimentally, and from these results a CHT diagram, useful to characterize the cure of the system, has been constructed in which the influences of both the underlying heating rate and the frequency are identified. A simulation has been made to model the non-isothermal reaction kinetics of a thermoset in which vitrification and devitrification intervene, from which the theoretical dependence on frequency of the dynamic vitrification and devitrification times and temperatures has been established. A close correspondence between the results of the simulation and the experimental TOPEM data has been observed. Some apparent discrepancies in the devitrification times, particularly for the slowest heating rates, are attributed to relaxation effects occurring during the lengthy period during which the system remains in a vitrified state close to its glass transition temperature.

Acknowledgements

The authors are grateful for the provision of equipment, financial support and technical advice from *Mettler-Toledo*. J. M. H. is grateful for a Ramón y Cajal research grant. This work was supported by a grant from the *Spanish Ministry of Education and Science*, Project MAT 2008-06284-C03-03/MAT. The authors are grateful to *Huntsman* for the provision of the Jeffamine D-230 curing agent.

References

1. S. Montserrat, *J. Appl. Polym. Sci.* **1992**, *44*, 545.
2. I. Fraga, S. Montserrat, J. M. Hutchinson, *J. Therm. Anal. Calorim.* **2008**, *91*, 687.
3. Van Assche, G.; Van Hemelrijck, A.; Rahier, H.; Van Mele, B. *Thermochim. Acta* **1996,** *286*, 209.
4. G. Van Assche, A. Van Hemelrijck, H. Rahier, B. Van Mele, *Thermochim. Acta* **1997**, *304/305*, 317.
5. B. Van Mele, G. Van Assche, A. Van Hemelrijck, *J. Reinforced Plastics and Composites* **1999**, *18*, 885.
6. S. Montserrat, J. G. Martín, *Thermochim. Acta* **2002**, *388*, 343.
7. S. Montserrat, F. Roman, P. Colomer, *J. Appl. Polym. Sci*. **2006**, *102*, 558.
8. G. Wisanrakkit, J. K. Gillham, *J. Appl. Polym. Sci.* **1991**, *42*, 2453.
9. J. E. K. Schawe, T. Hütter, C. Heitz, I. Alig, D. Lelliger, *Thermochim. Acta* **2006**, *446*, 147.

10. K. Chen, K. Harris, S. Vyazovkin, *Macromol. Chem. Phys.* **2007**, *208*, 2525.

11. S. Vyazovkin, K. Chen, *Chem. Phys. Letters* **2007**, *448*, 203.

12. I. Fraga, S. Montserrat, J. M. Hutchinson, *J. Therm. Anal. Calorim.* **2007**, *87*, 119.

13. S. Montserrat, *Polymer*, **1995**, *36*, 435.

14. I. Fraga. S. Montserrat, J. M. Hutchinson, *Macromol. Chem. Phys.* **2008,** 209, 2003.

15. M. R. Kamal, *Polym. Eng. Sci.* **1974**, *14*, 231.

16. J. P. Pascault, R. J. J. Williams, *J. Polym. Sci: Polym. Phys.* **1990**, *28*, 85.

17. M. L. Williams, R. F. Landel, J. D. Ferry, *J. Am. Chem. Soc.* **1955**, *77*, 3701.

18. C. W. Wise, W. D. Cook, A. A. Goodwin, *Polymer* **1997**, *38*, 3251.

19. E. Rabinowitch, *Trans. Faraday Soc.* **1937**, *33*, 1225.

20. A. T. DiBenedetto, *J. Polym. Sci: Polym. Phys.* **1987**, *25*, 1949.

21. S. Montserrat, Y. Calventus, J. M. Hutchinson, *Polymer* **2005**, *46*, 12181.

22. J. M. Hutchinson, S. Montserrat, *Thermochim. Acta* **2001**, *377*, 63.

23. J. M. Hutchinson, *Prog. Polym. Sci.* **1995**, *20*, 703.

24. S. Montserrat, G. Andreu, P. Cortés, Y. Calventus, P. Colomer, J. M. Hutchinson, *J. Appl. Polym. Sci.* **1996**, *61*, 1663.

25. P. Cortés, S. Montserrat, J. M. Hutchinson, *J. Appl. Polym. Sci.* **1997**, *63*, 17.

26. Y. Calventus, S. Montserrat, J. M. Hutchinson, *Polymer* **2001**, *42*, 7081.

Text for "Table of Contents"

TOPEM, a new multi-frequency DSC technique from Mettler-Toledo, is used to investigate the vitrification and devitrification processes that occur during the non-isothermal cure of a thermosetting resin. In addition to their dependence on the heating rate, this technique permits their frequency dependence to be evaluated in a single scan, and leads to an interesting extension of the CHT cure diagram.

Graphic for "Summary" and for "Table of Contents"